International Journal of Pharmaceutics 418 (2011) 217–226

Contents lists available at ScienceDirect

International Journal of Pharmaceutics

journal homepage: www.elsevier.com/locate/ijpharm

Informatics calibration of a molecular descriptors database to predict solid dispersion potential of small molecule organic solids

Michael D. Moore, Peter L.D. Wildfong*

Duquesne University Graduate School of Pharmaceutical Sciences, 600 Forbes Ave., Pittsburgh, PA 15282, USA

ARTICLE INFO

Article history:
Received 20 December 2010
Received in revised form 15 May 2011
Accepted 1 June 2011
Available online 3 July 2011

Keywords:
Amorphous dispersion
In silico prediction
DSC
PXRD
Pair distribution function
Physical stability

ABSTRACT

The use of a novel, *in silico* method for making an intelligent polymer selection to physically stabilize small molecule organic (SMO) solid compounds formulated as amorphous molecular solid dispersions is reported. 12 compounds (75%, w/w) were individually co-solidified with polyvinyl pyrrolidone:vinyl acetate (PVPva) copolymer by melt-quenching. Co-solidified products were analyzed intact using differential scanning calorimetry (DSC) and the pair distribution function (PDF) transform of powder X-ray diffraction (PXRD) data to assess miscibility. Molecular descriptor indices were calculated for all twelve compounds using their reported crystallographic structures. Logistic regression was used to assess correlation between molecular descriptors and amorphous molecular solid dispersion potential. The final model was challenged with three compounds. Of the 12 compounds, 6 were miscible with PVPva (*i.e.* successful formation) and 6 were phase separated (*i.e.* unsuccessful formation). 2 of the 6 unsuccessful compounds exhibited detectable phase-separation using the PDF method, where DSC indicated miscibility. Logistic regression identified 7 molecular descriptors correlated to solid dispersion potential ($\alpha = 0.001$). The atomic mass-weighted third-order R autocorrelation index (R3m) was the only significant descriptor to provide completely accurate predictions of dispersion potential. The three compounds used to challenge the R3m model were also successfully predicted.

1. Introduction

The aqueous solubility of a small molecule organic (SMO) solid is one of the principal physicochemical properties considered when evaluating the developability of a new chemical entity (NCE) for pharmaceutical use. Although a number of chemically- and physically-based approaches are available for enhancing the apparent aqueous solubility of active pharmaceutical ingredients (API), it is still estimated that more than 40% of highly potent compounds fail to reach clinical trials due to the inability to overcome poor aqueous solubility (Kaushal et al., 2004). It is proposed that this statistic is somewhat inflated, not necessarily due to the inefficacy of available methods, but rather owing to the raw material requirements associated with empirically assessing the potential of each. During early preformulation studies many companies have only very small quantities (mg) of candidate API available for study; scientists are ultimately forced to investigate only a fraction of the existing technology, where unsuccessful outcomes may deem a therapeutically efficacious API undevelopable. The development of predictive models to optimize these methods in an attempt to preserve early stage raw material supplies is thus imperative.

Stabilization of an API as an amorphous solid phase through the formation of binary amorphous molecular solid dispersions has received increasing attention yielding up to a four-fold enhancement of apparent aqueous solubility relative to the crystalline form (Hancock and Parks, 2000). Binary amorphous molecular solid dispersions are created through the rapid co-solidification of an API and a pharmaceutically acceptable excipient, such as a polymer, at loadings sufficient to achieve a physically stable amorphous API. Due to the kinetic nature of the formation, spray drying (Janssens et al., 2008), super-critical fluid processing (Sethia and Squillante, 2004), lyophilization (Waard et al., 2008), and hot-melt extrusion (Chokshi and Zia, 2004) have all been successfully implemented in the preparation of amorphous molecular solid dispersions. Successful formation has been attributed to the presence of specific and/or nonspecific adhesive interactions (Huang et al., 2008; Taylor and Zografi, 1997), as well as antiplasticization effects intended to reduce molecular mobility (Mooter et al., 2001).

Predictive models for API:polymer miscibility have been introduced and are largely derived from solution thermodynamics. Lattice based solution models, such as Flory–Huggins theory, can be used to assess miscibility in API:polymer blends. In addition to developing methods for estimating the Flory–Huggins interaction parameter, Marsac (Marsac et al., 2006b) developed a model that predicted the solubility of an API in a polymer based on a

* Corresponding author. Tel.: +1 412 396 1543; fax: +1 412 396 4660.
E-mail address: wildfongp@duq.edu (P.L.D. Wildfong).

0378-5173/$ – see front matter © 2011 Elsevier B.V. All rights reserved.
doi:10.1016/j.ijpharm.2011.06.003

combination of interaction variables and Flory–Huggins theory. Janseens (Janssens et al., 2010) applied the similar theory to model solid dispersion preparation method effects on the solubility of API in polymer. Friesen et al. (2008) showed physical properties of APIs, such as hydrophobicity (*i.e.* log *P*), thermodynamic parameters (*e.g.* melting temperature) and kinetic parameters (*e.g.* glass transition temperature) to provide insight concerning formulation strategies for solid dispersion systems. In addition to ionic interactions, when applicable, Yoo et al. (2009) also observed a correlation between hydrophobicity values of APIs and miscibility with a given polymer. Despite the recent advances, explicit universal criteria for API:polymer miscibility are still lacking.

Quantitative structure property relationships (QSPR) were derived from the fundamental concept that a compound's behavior is a result of its chemical structure. In QSPR models, molecular descriptors, single integer indices that encode specific structural information for a given compound, are typically regressed against some physical, chemical, or mechanical property. Applications of molecular descriptors in QSPR modeling include predicting pharmacokinetic performance (Waterbeemd and Gifford, 2003), describing physical properties of alkanes (Estrada, 1996), and prediction of soil sorption coefficients of pesticides (Gramatica et al., 2000). Coupled with characterization techniques to classify the co-solidified composites containing a given API, molecular descriptors have the potential to provide insight to API:polymer miscibility using a materials informatics approach.

In this study, 12 model compounds were prepared by a melt-quench procedure using polyvinylpyrrolidone:vinyl acetate (PVPva) copolymer as a stabilizing agent with useful thermoplastic properties and the potential (*i.e.* miscibility) for generating an amorphous molecular solid dispersion. Each co-solidified sample was characterized by thermal analysis, powder X-ray diffraction (PXRD), and a pair distribution function (PDF) method recently introduced into the literature (Newman et al., 2008). Rather than attempting to quantify the extent of miscibility between API and polymer to afford a continuous dependent variable, each sample was classified as a successful formation (*i.e.* completely miscible) or an unsuccessful formation (*i.e.* partially miscible or immiscible) based upon conclusions drawn from the analyses. Complete miscibility, in the context of this work, is the ability of an API to form a unique phase when intimately mixed with a carrier material, where the unique phase is characterized by the formation of short range order possessing physical, structural, and other intrinsic properties distinct from either individual amorphous component. Molecular descriptors were calculated for each of the 12 model compounds comprising the library and tested for correlation to dispersion potential using logistic regression. A univariate model was created that predicted solid dispersion potential from a single molecular descriptor and challenged using three compounds not included in the calibration.

At the outset, it should be noted that the model developed herein is not proposed to be universally applicable across all SMO compounds, nor is it predictive of the time course of physical instability (*i.e.* devitrification). Rather, a significant portion of the discussion will attempt to highlight the limitations associated with the model and define the pertinent variance space for its applicability. The central objective of this work was to illustrate the potential of *in silico* calculations to create models that may one day provide the means for intelligent selection of stabilizing agents in the design of amorphous molecular solid dispersions. This possibility is ultimately afforded by the ability to classify co-solidified samples to compliment the interpretation that is possible from solid-state characterization methods alone.

2. Materials and methods

Cloperastine, terfenadine, propranolol, chlorpropamide, nifedipine, melatonin, and quinidine were all purchased from Sigma–Aldrich (St. Louis, MO). Ketoconazole and itraconazole were purchased from Spectrum (Gardena, CA). Indomethacin, cimetidine, and tolbutamide were purchased from MP Biomedicals (Solon, OH). Felodipine was purchased from Tecoland Corporation (Edison, NJ), sulfanilamide was purchased from Acros Organics (Geel, Belgium), bicalutamide was purchased from Altan (Orange, CT), and Kollidon VA64 (PVPva) was a gift from BASF (Ludwigshafen, Germany). All model and test compounds are shown in Table 1.

2.1. Solid dispersion and amorphous phase preparation

Solid dispersion samples were manufactured using a melt-quench method (Sekiguchi and Obi, 1961). Briefly, each API and PVPva was weighed and dispensed into a scintillation vial at 75 wt% API loading. The powders were physically mixed for a period of 5 min by manual agitation. To avoid sub-sampling, the entire mixed sample was added to a crucible heated in a silicone oil bath. The oil bath was maintained at a temperature equal to the fusion temperature of the API ($T_{f,API}$) + 10 °C. In the instance where $T_{f,API}$ was less than 150 °C (*e.g.* the temperature at which PVPva liquefies), the mixture was held isothermally at 160 °C. The isothermal hold time was between 10 and 20 min to provide sufficient time for mixing. The hold time was determined using thermogravimetric analysis and was defined as the time (at a given preparation temperature) where ≥2% weight loss occurred. The molten mixture was subsequently quenched in an ice water bath. Amorphous samples of each component were produced by holding the crystalline API above its melting temperature for approximately 10 min followed by quenching in an ice bath. The melt-quench samples were removed from the crucible intact and examined. All preparations were repeated twice ($n = 3$).

2.2. Differential scanning calorimetry (DSC)

Glass transition temperatures (T_g) for amorphous preparations of each model compound, PVPva, and the co-solidified samples were measured using a Model Q100 DSC (TA Instruments, New Castle, DE) under constant nitrogen purge (~50 mL/min). A three-point temperature calibration was performed at 20 °C/min using o-terphenyl, indium, and tin standards. The cell constant calibration was performed at 20 °C/min using indium. In an attempt to reduce artifacts arising from sample preparation procedures (*i.e.* grinding), approximately 5 mg intact "sample chips" were hermetically sealed in aluminum pans. To normalize thermal history, samples were first heated at 20 °C/min to 105 °C, held isothermally for 2 min, and subsequently cooled to −20 °C at 20 °C/min. Samples were then cycled from −20 °C to 120 °C at 20 °C/min for T_g determination.

The expected T_g assuming an intimate mixture was calculated using the Couchman–Karasz (Couchman and Karasz, 1978) equation given by:

$$T_g = \frac{w_{API} T_{gAPI} + K w_p T_{gp}}{w_{API} + K w_p} \quad (1)$$

where w_{API} and w_p are the weight fractions of API and polymer, respectively, T_{gAPI} and T_{gp} are the glass transition temperatures of amorphous API and polymer, respectively, and $K = \Delta C_{pp}/\Delta C_{API}$, where ΔC_{pp} and ΔC_{pAPI} are the heat capacity step change through the glass transition region of the polymer and API, respectively. Experimental T_g values were determined from the measured DSC heat flow signal as the onset of the step change in heat capacity.

Table 1
Molecular structures and Cambridge Structural Database refcodes for compounds used in this study.

Compound CSD Code Model/Test	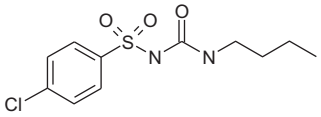 Chlorpropamide BEDMIG02 Model	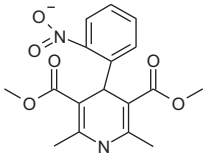 Nifedipine BICCIZ Model	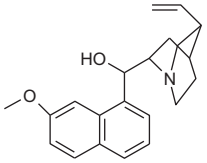 Quinidine BOMDUC Model
Compound CSD Code Model/Test	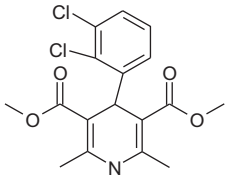 Felodipine DONTIJ Model	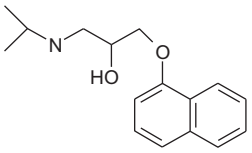 Propranolol FIDGAB Model	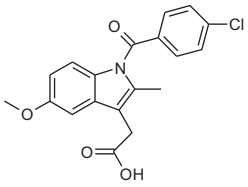 Indomethacin INDMET03 Model
Compound CSD Code Model/Test	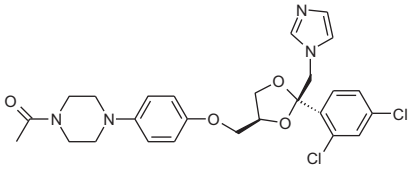 Ketoconazole KCONAZ Model	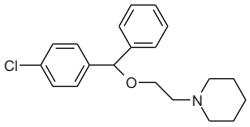 Cloperastine QAWNAD Model	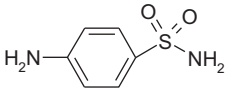 Sulfanilamide SULAMD06 Model
Compound CSD Code Model/Test	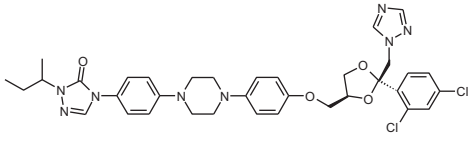 Itraconazole TEHZIP Model	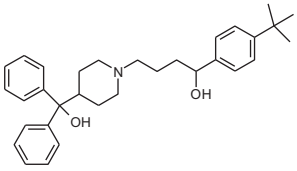 Terfenadine XUHTID Model	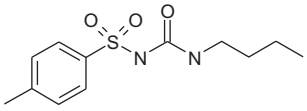 Tolbutamide ZZZPUS02 Model
Compound CSD Code Model/Test	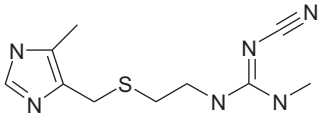 Cimetidine CIMETD Test	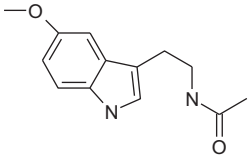 Melatonin MELATN01 Test	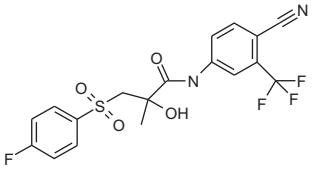 Bicalutamide JAYCES Test
Compound	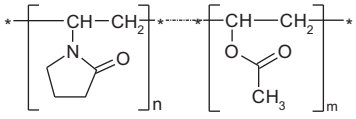 PVPva		

2.3. Powder X-ray diffraction (PXRD)

The PXRD data were collected in transmission geometry using an X'Pert Pro MPD system (PANalytical B.V., Almelo, the Netherlands) equipped with a copper anode ($\lambda = 1.5406$ Å), an auxiliary elliptical mirror, and X'Celerator™ detector. The operational voltage and amperage were set to 45.0 kV and 40.0 mA, respectively. Diffraction patterns were acquired on intact samples, sandwiched between two layers of Kapton® film and subsequently placed on a spinning vertical sample stage (16 rpm). Experimental parameters include an irradiation time of 51.04 s per step and an angular step size of 0.017°2θ over a 2–100°2θ range.

2.4. Pair distribution function (PDF)

The PDF is a total scattering method that exploits the Fourier relationship between X-ray diffraction intensity and the real-space arrangement of atoms, given appropriate data treatment (Egami and Billinge, 2003; Warren, 1990). The PDF gives the probability of finding atom pairs separated by a distance r, and is obtained by Fourier transform of the reciprocal space structure function, $S(Q)$, according to:

$$G(r) = \frac{2}{\pi}\int_0^{Q_{max}} Q[S(Q) - 1]\sin(Qr)\,dQ \quad (2)$$

where $S(Q)$ is the structure function obtained from a diffraction experiment and Q is the magnitude of the scattering vector. The term Q_{max} is the momentum transfer resolution of the diffraction experiment, which is dependent on the wavelength of radiation used and the maximum diffraction angle (°2θ) of data collection. Corrections consistent with those outlined by Egami and Billinge (2003) were made to the measured diffraction data leading to the calculation of the structure function. All intensity corrections (*e.g.* background due to Kapton® film scattering, absorption, *etc.*) and PDF calculations were performed using software developed in-house in the Matlab programming environment (v7.1, MathWorks,

Natick, MA) based on published equations (Egami and Billinge, 2003; Warren, 1990). The PDF transforms were optimized using the G_{low} quality criteria introduced by Peterson (Peterson et al., 2003).

The PDF has been shown to be useful in characterizing co-solidified composite samples in differentiating phase-separated from completely miscible systems (Ivanisevic et al., 2009; Newman et al., 2008). Briefly, the PDF transform for a co-solidified sample is compared to the linear combination of the PDF transforms obtained for each amorphous component comprising it. Scaling coefficients are multiplied by the amorphous component PDFs and serve as estimates of each component concentration in the co-solidified product. If the linear combination of the PDF for each amorphous component describes the PDF of the co-solidified sample, it is reasonable to conclude the system is at least partially phase-separated, as short-range order (*i.e.* the static local structure) of the co-solidified product can be described by the intrinsic distances found in the amorphous API and polymer. Large deviations between the calculated PDF determined by linear combination of the PDFs for the individual amorphous components and the PDF of the co-solidified sample are indicative of short-range order not presented in the individual components (*i.e.* that of a unique packing pattern). A statistically-founded protocol based on principles of error propagation has recently been introduced to aid in drawing conclusions from the aforementioned method (Moore et al., 2010). A sum-of-squares difference, *R*, between the calculated PDF and PDF of co-solidified sample was also determined for comparative purposes (Prince, 2004).

2.5. Molecular descriptors

The term molecular descriptor refers to a broad class of indices calculated under the principal objective of representing a 3-dimensional molecule as a simple number(s). Their successful use in QSPR studies, relating the structure of a compound to how it behaves, provides impetus to modeling amorphous molecular solid dispersion potential. By employing graph theory (Mihalic and Trinajstic, 1992), a branch in discrete mathematics dealing with the way objects are connected and the consequences of connectivity, single integer indices may be calculated that encode structural information for a given molecule. Molecular graphs are a 2-dimensional depiction of molecules, where atoms are represented by vertices and bonds by edges. Two molecular graphs are isomorphic if there is a one-to-one correspondence between their vertex sets and edge sets. For a given molecular graph, *U*, a graph invariant is a quantity that has the same value for any graph that is isomorphic with *U* (Mihalic and Trinajstic, 1992).

From the molecular graph, important theoretical matrices may be calculated. The vertex-adjacency matrix is a square symmetric matrix having off-diagonal values of one for adjacent vertices and zero for non-adjacent vertices. Similarly, the edge-adjacency matrix is a square symmetric matrix having off-diagonal values of one for adjacent edges and zero for non-adjacent edges. The distance matrix is a square symmetric matrix having off-diagonal values describing the shortest topological distance between two vertices. Single integers may be obtained from the mathematical manipulation of these matrices, thereby generating a class of molecular descriptors called topological indices. These indices are graph invariants and do not possess atom identities, thereby lacking heteroatom differentiation and stereochemical features of the molecule (Estrada, 1996).

To combat this issue, indices are calculated from weighted graph invariants, where atomic mass, atomic number, van der Waals volumes, and atomic polarization constants have all been implemented. These descriptors are much more powerful and have seen an increased exposure in structure-property relationships studies. In this study, molecular descriptors were calculated using the EDRAGON online program (2002, 2005, Tetko et al., 2005). Three-dimensional coordinates and atom connectivity was obtained from the Cambridge Structural Database (CSD) (Allen, 2002; Thomas et al., 2010), where the CSD code for each model and test compound are listed in Table 1.

2.6. Logistic regression

The intent of this study was to introduce a novel method for modeling the potential of a compound to successfully form an amorphous molecular solid dispersion with PVPva using a common method of preparation. Attempting to develop a method to quantify the extent of miscibility between API compounds and PVPva would likely confound the results of the analysis, as errors in this determination would propagate into the regression modeling. Therefore, the response in this analysis is a discrete, dichotomous variable taking a value of 1 for successful formation of an amorphous molecular solid dispersion (*i.e.* completely miscible) or a value of 0 for unsuccessful formation (*i.e.* partially miscible or immiscible) based upon conclusions drawn from the analyses. The inclusion of a dichotomous dependent variable unfortunately violates many of the assumptions of general linear regression (Kleinbaum et al., 1998). Logistic regression was, therefore, used for modeling purposes in this study.

Logistic regression was performed using maximum likelihood (ML) estimation to calculate the regression coefficient for each molecular descriptor. Initial regression coefficients are estimated and the ML is calculated. The regression coefficient is iteratively adjusted until the maximum value of the ML (Eq. (3)) is achieved. To avoid multiplication of probabilities, the natural logarithm of the ML function is used, and given by:

$$\ln(\mathrm{ML}) = \sum [Y_i * \ \ln P_i] + [(1 - Y_i) * \ln(1 - P_i)] \tag{3}$$

where Y_i is the observed value (*i.e.* 0 or 1) and P_i is the estimated probability as obtained by:

$$P_i = \frac{e^{b_0 + b_1 X_i}}{1 + e^{b_0 + b_1 X_i}} \tag{4}$$

where $b_0 + b_1 X_i$ is the general linear model (Kleinbaum and Klein, 2002; Pampel, 2000; Pregibon, 1981). The effect of individual variables on model significance was tested by comparing the change in deviance (*D*), which is Eq. (3) multiplied by −2. The likelihood ratio (LR) test statistic, corresponds to the arithmetic difference between the deviance values for two models (*e.g.* with and without a particular variable included), and follows a χ^2 distribution. The significance of the calculated regression coefficient for each molecular descriptor was evaluated by comparing the reduction of deviance value of the full model against using only the model intercept.

The robustness of the calibration was assessed using the leave-one-out (LOO) cross-validation method. Briefly, one of the compounds comprising the calibration library was removed from the data set. The remaining compounds were used to construct a calibration and a subsequent prediction on the compound removed from the library was performed. This was iteratively repeated for all compounds, where the sum of the total error was reported.

3. Results

3.1. Co-solidified sample characterization

Amorphous molecular solid dispersions are formed as a result of the miscibility between the components comprising the sample. To enable model estimation, interpretations from DSC and PDF

Table 2
DSC and PDF analyses results.

	DSC analysis			PDF analysis			Conclusion
	Ideal T_g (°C)	T_{g1} (°C)	T_{g2} (°C)	R value	Drug conc. (w/w)	Polymer conc. (w/w)	
Felodipine:PVPva	64.6	64.9	–	0.2126	0.81	0.19	Miscible
Quinidine:PVPva	79.7	59.7	81.9	0.0689	0.73	0.27	Phase-separated
Terfenadine:PVPva	79.1	60.6	–	0.0864	0.73	0.27	Phase-separate

analyses were used to classify the co-solidified samples as either miscible or phase-separated. An examination of interpretations drawn from the analyses will be presented for three of the calibration compounds. The first example will illustrate a co-solidified sample categorized as an amorphous molecular solid dispersion, the second will detail identification of a phase-separated system according to both DSC and PDF results, and the final will showcase a phase-separated system identified by PDF results. A compilation of calculated parameters associated with each example are given in Table 2.

The DSC thermogram for amorphous felodipine, PVPva, and the 75 wt% co-solidified sample is shown in Fig. 1a. A single T_g at 64.9 °C was observed for the co-solidified sample. The PDF analysis and respective difference plot for this system is shown in Fig. 1b. From Table 2, the calculated T_g for an ideal 75 wt% mixture is 64.6 °C, which is in good agreement with the experimentally determined 64.9 °C shown in Fig. 1a. The difference plot for the PDF analysis (Fig. 1b) exhibits regions in r where the confidence intervals do not contain zero. An R of 0.2126 (Table 2) corresponds to 21% error between the two PDF patterns. Refined API and polymer concentrations (scaling coefficients) of 0.81 and 0.19 (Table 2) deviate substantially from theoretical concentrations of 0.75 and 0.25, respectively. Based on a single T_g and the large deviations between the calculated and measured PDF of the co-solidified sample, the system is an amorphous molecular solid dispersion.

The DSC thermogram for amorphous quinidine, PVPva, and the 75 wt% co-solidified sample is shown in Fig. 2a. Glass transition events at 59.7 °C and 81.9 °C were observed for the co-solidified sample. Although the DSC results alone provide conclusive evidence of phase-separation, the PDF analysis was performed, and is shown in Fig. 2b. The difference plot (Fig. 2b) for the PDF analysis shows confidence intervals that contain zero through the entire r region. In addition to this, a satisfactory R value of 0.0689 and refined API and polymer concentrations of 0.73 and 0.27 (Table 2), respectively, were also observed. The system is phase-separated based on evidence of two T_g events and the agreement between the calculated and measured PDF for the co-solidified sample.

The DSC thermogram for amorphous terfenadine, PVPva, and the 75 wt% co-solidified sample is shown in Fig. 3a. A single T_g event at 60.6 °C was observed for the co-solidified sample, albeit relatively close to the T_g observed for the amorphous terfenadine. The difference plot (Fig. 3b) for the PDF analysis shows confidence intervals that ultimately contain zero through the entire r region. In addition to this, a low R and refined concentration values (Table 2) that are close to the theoretical concentrations were also observed. It is concluded that the system is phase-separated as a result of a single T_g value near that of the amorphous API, and the good agreement between the calculated and measured PDF for the co-solidified sample.

The final results of the co-solidified sample analyses are listed in Table 3. Of the 12 compounds comprising the calibration library, DSC and PDF analyses revealed six successfully formed an amorphous molecular solid dispersion (*i.e.* miscible with PVPva) and six formed phase separated systems. Propranolol, cloperastine, and sulfanilamide all exhibited Bragg diffraction peaks (PXRD analysis), a clear indication of phase separation, following preparation. Nifedipine and terfenadine both displayed a

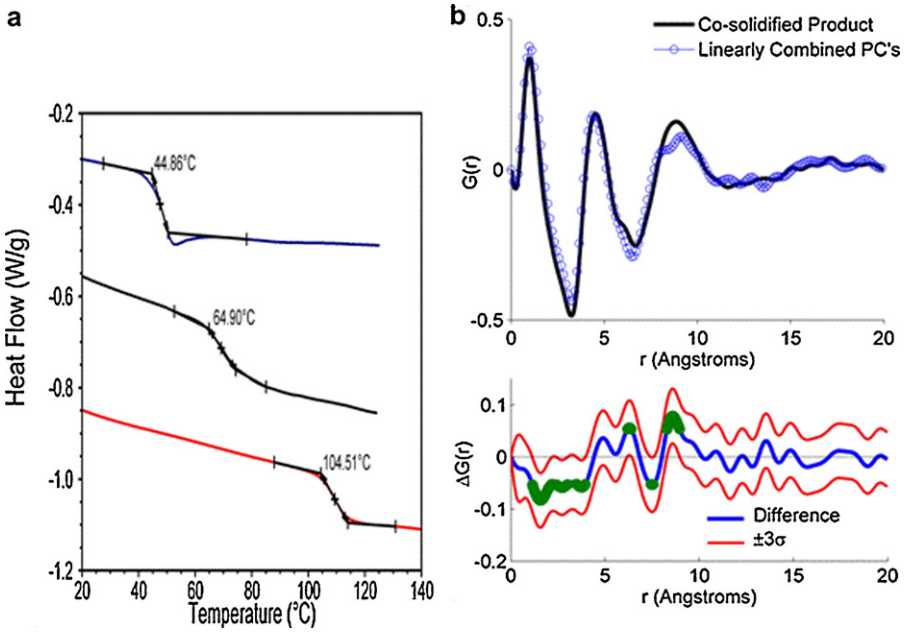

Fig. 1. (a) DSC thermogram for amorphous felodipine (blue), PVPva (red), and 75 wt% co-solidified product (black); (b) PDF analysis (as labeled). (For interpretation of the references to color in this figure legend, the reader is referred to the web version of the article.)

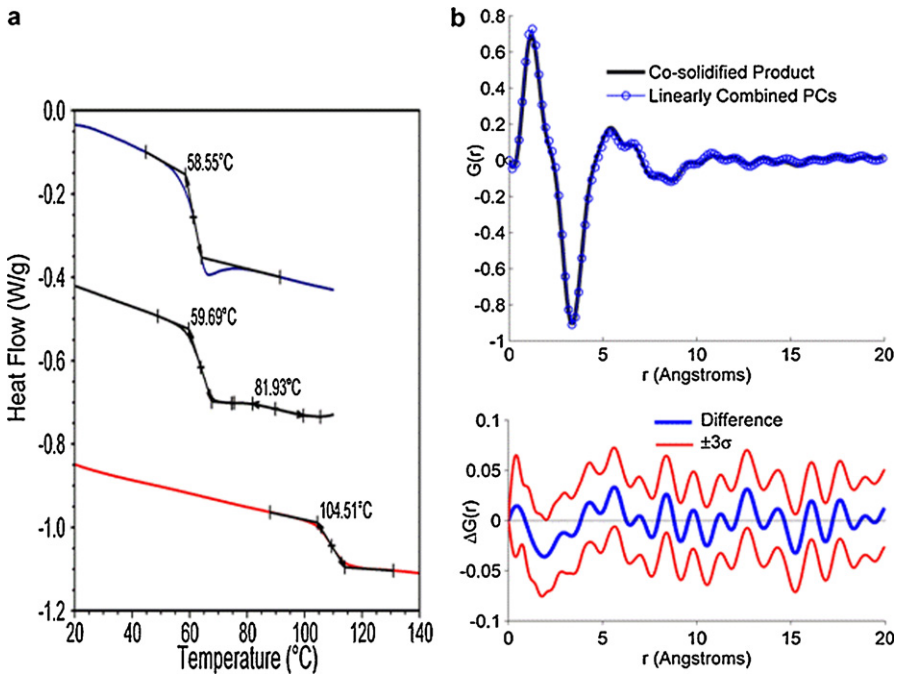

Fig. 2. (a) DSC thermogram for amorphous quinidine (blue), PVPva (red), and 75 wt% co-solidified product (black); (b) PDF analysis (as labeled). (For interpretation of the references to color in this figure legend, the reader is referred to the web version of the article.)

single T_g but were shown to be phase-separated using the PDF analyses.

3.2. Calibration

Univariate logistic regression was performed by estimating regression coefficients for each of the calculated molecular descriptors. Subsequently, a model containing the regression coefficient for a given molecular descriptor was compared with a model containing only the mean using the LR test statistic. From this metric, the significance of the descriptor was determined. Molecular descriptors having a significance ≥0.999 (*i.e.* $\alpha = 0.001$) were retained for further analysis. The results of the univariate screening are given in Table 4. Along with the regression equation, deviance, LR, and error of cross-validation are shown. From each of these parameters, the atomic mass-weighted third-order R autocorrelation index, R3m, appears to be the most significant. Other significant molecular descriptors include the topological distance between oxygen and chlorine atoms (T(O···Cl)), the sum of the eigenvalues of an atomic number-weighted distance matrix (SEigZ), the sum of the eigenvalues of an atomic mass-weighted distance matrix (SEigm), first-order H autocorrelation weighted by atomic mass (H1m), the total H autocorrelation weighted by atomic mass (HTm), and the maximum of the fourth-order

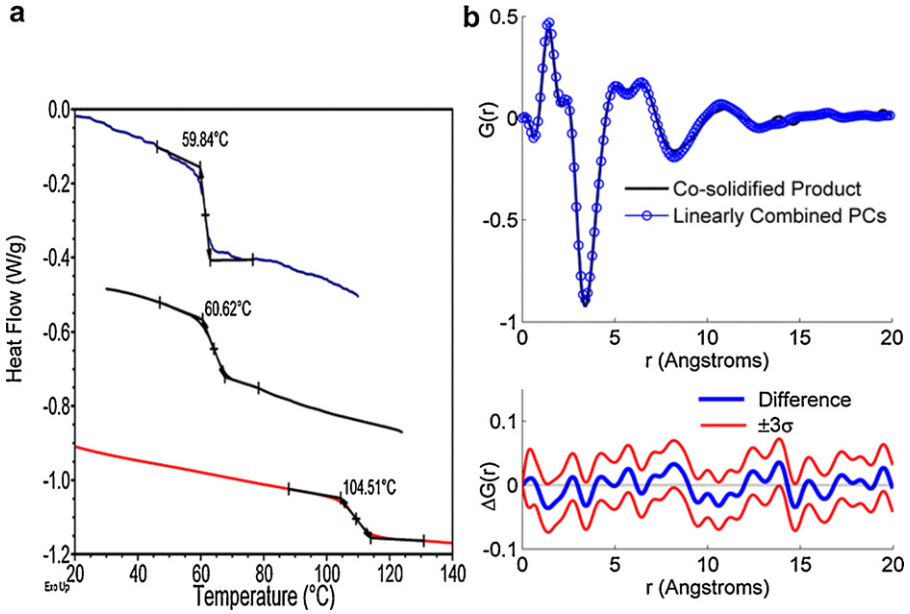

Fig. 3. (a) DSC thermogram for amorphous terfenadine (blue), PVPva (red), and 75 wt% co-solidified product (black); (b) PDF analysis (as labeled). (For interpretation of the references to color in this figure legend, the reader is referred to the web version of the article.)

Table 3
Calibration library generation results.

Compound	Miscible?	Comments
Felodipine	Yes	–
Indomethacin	Yes	–
Ketoconazole	Yes	–
Itraconazole	Yes	Could not obtain amorphous itraconazole; no PDF test
Tolbutamide	Yes	–
Chlorpropamide	Yes	–
Nifedipine	No	PDF confirmation only; crystallinity day 1 for repeats
Quinidine	No	Detectable phase separation from DSC and PDF
Propranolol	No	Detectable crystallinity (PXRD) on day 1
Cloperastine	No	Detectable crystallinity (PXRD) on day 1
Terfenadine	No	PDF confirmation only; crystallinity day 1 for repeats
Sulfanilamide	No	Detectable crystallinity (PXRD) on day 1

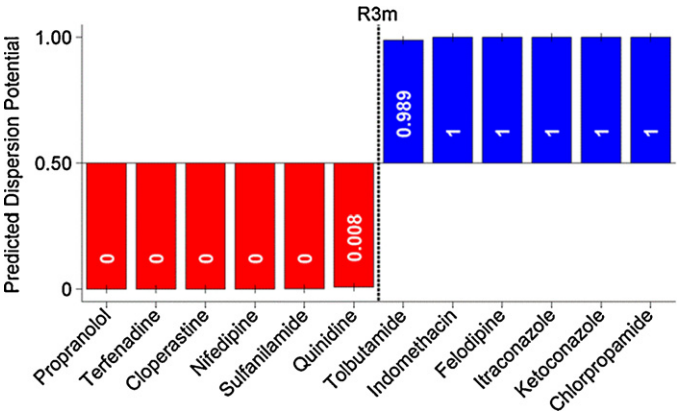

Fig. 4. Predicted dispersion potential probabilities for each of the 12 model compounds. Red indicates a correct prediction for unsuccessful formation and blue indicates a correct prediction for successful formation. (For interpretation of the references to color in this figure legend, the reader is referred to the web version of the article.)

R autocorrelation weighted by atomic mass (R4m+). The R3m index will be described in detail later; however, an explanation of other indices is beyond the scope of the paper and interested readers are directed elsewhere (Todeschini and Consonni, 2002).

Following univariate screening, both forward and backward elimination multivariate screening were performed at a significance level of 0.8 (*i.e.* $\alpha = 0.2$). The R3m index was the only remaining variable, and therefore, served as the final model. Predicted probabilities of amorphous molecular solid dispersion potential using the R3m model are shown graphically in Fig. 4. The results from testing the R3m model with three compounds not used in the calibration are shown schematically in Fig. 5. A description of the R3m index and explanation of its potential significance will be addressed in the discussion section.

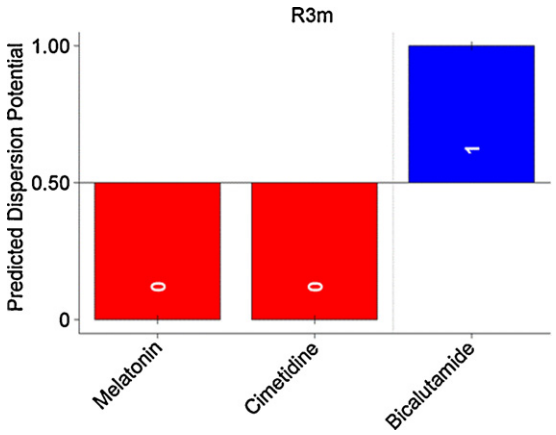

Fig. 5. Predicted dispersion potential probabilities for each of the 3 test compounds. Red indicates a correct prediction for unsuccessful formation and blue indicates a correct prediction for successful formation. (For interpretation of the references to color in this figure legend, the reader is referred to the web version of the article.)

4. Discussion

As stated in the introduction, the central objective of this research was to illustrate the potential of using *in silico* molecular calculations to create predictive models for assessing miscibility between a compound and polymeric material, afforded by the ability to classify co-solidified samples using advanced solid-state characterization methods. A further interpretation of this hypothesis states that some underlying molecular property is responsible for its ability to form a unique phase when intimately mixed with a carrier material. It is assumed that API:polymer miscibility is represented by the formation of short range order possessing physical, structural, and other intrinsic properties distinct from either individual amorphous component. It is further assumed that a completely miscible system will need to undergo phase separation as a pre-requisite to crystallization. The extent of miscibility between a given compound and polymer is sensitive to many different variables. The method of preparation, drug loading, and environmental factors may all affect the outcome of this determination. Conclusions concerning miscibility in this study will be with reference to the melt-quench method used, the fixed concentration range interrogated, and assumptions (*i.e.* statistical significance of interpretations) derived from direct observation of characterization data.

4.1. Co-solidified sample characterization

Although DSC and the PDF technique are often complementary, instances occur when results are contradictory. It is recognized that, in theory, the DSC sample will be structurally different from the PDF sample in this study due to the thermal normalization step in the DSC procedure. Since the time interval between co-solidified sample preparation and sample analysis is short, it is assumed that the amount of structural annealing in the PDF sample is negligible.

Table 4
Model parameters for the seven best univariate models.

Molecular descriptor	Regression equation	Deviance	LR	LOO CV
T(O···Cl)	logit $P(Y) = -1.927 + 0.208$T(O···Cl)	6.513	10.86	0.3841
SEigZ	logit $P(Y) = -12.33 + 7.37$SEigZ	4.889	12.49	0.4208
SEigm	logit $P(Y) = 12.57 + 7.50$SEigm	4.813	12.56	0.4199
H1m	logit $P(Y) = -17.78 + 12.31$H1m	6.314	11.06	0.3964
HTm	logit $P(Y) = -13.25 + 1.14$HTm	5.992	11.39	0.3720
R3m	logit $P(Y) = -88.54 + 135.18$R3m	0.039	17.34	0.0565
R4m+	logit $P(Y) = -15.2 + 346.22$R4m+	3.253	14.12	0.2637

In the first example, a single T_g (Fig. 1a, black line) intermediate to each of the amorphous component T_g events was observed for the co-solidified felodipine:PVPva sample. Since the experimental T_g of 64.9 °C is relatively close to the predicted 64.6 °C (Table 2), this may support classification as an amorphous molecular solid dispersion on its own accord.

Instances arise where DSC may not be sensitive to the presence of multiple T_g events. Possible explanations include convolution of two T_g events into a single T_g, the magnitude of the heat capacity change associated with an additional phase(s) is below the sensitivity of the instrument, the T_g event is superimposed over some other thermal transition, or the glass transition event unexpectedly occurs outside of the temperature range interrogated. In addition, heating the sample during the measurement may consequently force miscibility in a phase separated system. Each instance warrants the application of an alternative characterization technique, such as the PDF method using error propagation estimates, to examine the co-solidified sample.

For the felodipine:PVPva co-solidified sample, the high R value of 21.26%, concentrations inconsistent with theoretical values, and the presence of confidence intervals for r-values not containing zero (Fig. 1b and Table 2) all serve as indicators that the co-solidified product exhibits a packing pattern different than that produced by the local structure of each individual amorphous component. From Fig. 1b, the difference plot indicates a significant difference between the calculated PDF and the co-solidified PDF around 8–9 Å.

The limitations imposed by using Cu Kα radiation call for considering the distributions of delta peaks in the convoluted probability peaks. Distribution changes manifest as alterations to the shape of the probability peak, as observed for the felodipine:PVPva co-solidified sample (Fig. 1b, black line) relative to the combine amorphous components (Fig. 1b, blue circles). It may be concluded that this sample has unique interatomic distances formed around 8–9 Å not found in either amorphous component, and therefore, is an amorphous molecular solid dispersion. This conclusion is consistent with those found elsewhere (Rumondor and Taylor, 2010).

In the second example, the thermogram of the quinidine:PVPva co-solidified sample (Fig. 2a, black line) displays a T_g event near that of the amorphous quinidine (Fig. 2a, blue line) and a second intermediate to each amorphous component. The substantial depression of the polymer T_g event is likely a consequence of partial miscibility (concentration dependent) between quinidine and PVPva. The presence of a detectable T_g for the amorphous drug in the co-solidified product is probably the excess drug existing as an independent amorphous phase. Given the detection of two T_g events, it is reasonable to conclude that the co-solidified sample has phase-separated. From Fig. 2b, agreement between the calculated PDF and the co-solidified sample was obtained as evidenced in the difference plot. The inclusion of zero throughout the entire r range, low R value, and experimentally determined concentration values close to theoretical (Table 2) all support the conclusion of phase separation.

The final example is unique owing to the disagreement in conclusions drawn from each characterization technique. In Fig. 3a, the thermogram for the terfenadine:PVPva co-solidified sample (black line) shows a single detectable T_g of 60.6 °C close to the T_g of 59.8 °C for amorphous terfenadine (blue line). Although this likely indicates the presence of amorphous terfenadine, a definitive conclusion is, unfortunately, not readily available.

In Fig. 3b, the linearly combined amorphous component PDF patterns are superimposed over the co-solidified sample PDF. From the difference plot, it is shown that the confidence intervals include zero throughout the entire range of r values. Additionally, the refined concentration values and low R value (Table 2) indicate a good fit between the two PDF patterns. The aforementioned PDF data supports the conclusion that the terfenadine:PVPva co-solidified sample is phase-separated.

Table 3 summarizes miscibility determination between the 12 model compounds comprising the calibration library and PVPva, where a few noteworthy points deserve some discussion. Propranolol, cloperastine, and sulfanilamide all exhibited Bragg diffraction peaks in PXRD patterns obtained following co-solidification, thereby indicating phase separation. Nifedipine and terfenadine were identified as phase-separated using the PDF method, and their respective thermograms for co-solidified samples displayed single T_g events. This conclusion was indirectly confirmed when the repeat co-solidification samples were analyzed. In their subsequent preparations, PXRD patterns from both compounds displayed Bragg diffraction peaks immediately following sample preparation, thereby corroborating the previous conclusions.

Evaluation of itraconazole indicated that it successfully formed an amorphous molecular solid dispersion with PVPva. From Table 3, amorphous itraconazole was not obtainable, thereby preventing the PDF analysis; a shortcoming of the PDF method. It may be expected that making conclusions solely on DSC data increases the probability of a misclassification. In the previous discussion, terfenadine and nifedipine were classified as phase separated by PDF analysis. It was shown that subsequent preparations were prone to different levels of devitrification as evidenced in PXRD analyses. The inability to procure amorphous itraconazole was attributable to the tendency for instantaneous crystallization upon quench cooling. Given this characteristic, phase-separated itraconazole is expected to instantaneously crystallize upon quenching. Three different itraconazole:PVPva preparations consistently produced a single T_g event with PXRD patterns lacking any detectable Bragg diffraction. The combination of all information supports a classification of complete miscibility between itraconazole and PVPva, which is further founded on conclusions drawn elsewhere (Six et al., 2004).

4.2. Calibration

From Table 4, the most promising molecular descriptor appears to be the R3m index. Deviance is the natural logarithm of the likelihood value multiplied by −2, and serves as an estimate of error. As the deviance approaches zero, and is minimized, the predictions approximate experimental values and the model becomes more significant. The deviance for the R3m model (0.039) is two orders of magnitude lower than that of the next best index. The LR approximates a χ^2 statistic, where a larger value is indicative of greater significance. The R3m index has the greatest LR value for all molecular descriptors tested. Finally, the error of cross-validation (LOO CV) is a metric for determining the robustness of the model. By iteratively removing a compound from the library, creating a calibration, making a prediction on the compound removed, and calculating the error, the extent to which each sample influences the calibration is assessed. The LOO CV for the R3m is an order of magnitude less than that of the next best value, thereby confirming the robustness of the R3m model.

It is important to consider the possibility of over-saturating a model constructed from only 12 samples. With this in mind, multivariate logistic regression at a significance level of $\alpha = 0.2$ was performed. Both forward- and backward-elimination yielded the same conclusion; the R3m index was the single most significant descriptor. Shown in Fig. 4 are the R3m predicted probabilities for each calibration sample with an estimated confidence interval in bar graph form. Interestingly, 10 of the 12 compounds were predicted perfectly (to four decimal places), while quinidine and tolbutamide only slightly deviated. The estimated confidence

intervals ($\alpha = 0.05$) for all 12 predictions indicated the predictions are reliable.

The R3m index is part of a class of molecular descriptors known as GETAWAY (Geometry, Topology, and Atom-Weights AssemblY) (Consonni et al., 2002a,b). The GETAWAY indices link 3D geometry to atom relatedness, while retaining specific chemical information. The first part of calculating any GETAWAY descriptor is to calculate the molecular influence matrix, **H**, given by:

$$\mathbf{H} = \mathbf{M} \cdot \text{inv}(\mathbf{M}'\mathbf{M}) \cdot \mathbf{M}' \quad (5)$$

where **M** is the molecular matrix comprised of A rows (number of atoms in molecule) and three columns (Cartesian atomic coordinates). The molecular influence matrix is equivalent to a leverage matrix, ostensibly describing the Euclidean distance of atoms from the geometric center of the molecule. The diagonal elements of **H**, h_{ii}, are called leverages and represent the "influence" of each atom in determining the whole shape of the molecule. Interestingly, lower leverages are found for atoms in molecules of spherical shape, while higher leverages for atoms in more linear compounds. Each off-diagonal element of **H** represents the accessibility of the ith atom to interactions with the jth atom, where negative elements represent a low degree of accessibility. From the molecular influence matrix, various R-GETAWAY descriptors can be calculated, including the w-weighted kth order autocorrelation index, $R_k(w)$, given by:

$$R_k(w) = \sum_{i=1}\sum_{j>1} \frac{\sqrt{h_{ii}h_{jj}}}{r_{ij}} \cdot w_i \cdot w_j \cdot \delta(k; d_{ij}) \quad k = 1, 2, \ldots, d \quad (6)$$

where h is the element of the molecular influence matrix, r is the geometric interatomic distance, w is the chemical weighting, k is the path length, d is the topological interatomic distance, and δ is equal to 1 when $k = d$ and 0 when $k \neq d$. From this equation, the R3m descriptor may be interpreted as follows: "R"-GETAWAY "3rd"-order autocorrelation index weighted by the atomic mass, "m" (Consonni et al., 2002a).

A direct physical interpretation of the correlation between the R3m index and amorphous molecular solid dispersion potential is not readily apparent. From equation 6, some key conceptual attributes of this index are evident. Larger values are obtained for two peripheral atoms (*i.e.* further from the geometric center of the molecule) that are in close proximity to each other (r_{ij}). Additionally, as the atomic masses of the two atoms increase, so does the index; ultimately attributable to a larger number of electronegative atoms (*i.e.* oxygen, sulfur, chlorine) in SMO compounds. In this study, it was observed that as the index increases, the probability of successful solid dispersion formation increases, as well. From the previous discussion of the R3m index, it is reasonable to state that a molecule having electronegative atoms along its periphery that are conformationally positioned such that their interatomic distances are minimized results in an increased probability of dispersion formation.

One of the most intriguing comparisons is that of felodipine and nifedipine. Commonly prescribed calcium channel blockers, their structural similarities are readily apparent in Table 1. It has been previously reported that the nucleation rate in amorphous nifedipine, both as a pure phase and as a 3 wt% amorphous molecular solid dispersion with PVP, is substantially greater than that of felodipine in the equivalent state (Marsac et al., 2006a). In this study, felodipine was shown to be completely miscible with PVPva, whereas the co-solidified product of nifedipine and PVPva exhibited detectable phase separation. The benzene flanking the dihydropyridine in nifedipine contains a nitro group, where the same benzene contains two chlorine atoms in felodipine (Table 1). This substituent change causes a marked increase in the R3m index from 0.579 for nifedipine to 0.813 for felodipine.

Since the R3m includes specific information concerning 3D molecular geometry provided by the molecular influence matrix, atom relatedness by molecular topology, and chemical information by using the atomic mass weighting scheme, it is difficult to simplify the relationship between this sophisticated index and the mechanism of API:polymer miscibility. The mere increase in the R3m index can be attributable to multiple molecular features (*i.e.* increasing amount of electronegative atoms, large number of atoms distant to the geometric center, or intramolecular interactions three topological units apart). Any further extrapolation, at present, concerning this correlation would be speculative, and is the subject of ongoing research.

The R3m model was challenged with three compounds not used in the calibration. The results are shown in Fig. 5 as a bar plot. Both cimetidine and melatonin were accurately predicted to not form an amorphous molecular solid dispersion with PVPva. Dispersion formation for bicalutamide, however, was accurately predicted, and complete miscibility with the polymer was confirmed. It was important, when selecting compounds to test the model, that molecular attributes did not exceed the variance space of the molecules used to construct the calibration. For example, the fusion temperature for compounds included in the calibration fell in the range of 120–180 °C. Predictions for molecules having fusion temperatures substantially deviating from this range tended to be incorrect.

As with any materials informatics calibration, the power of the model increases with the variance spanned by the samples comprising it. Since this calibration contained only 12 compounds, it may seem that the variance space is relatively small. It is anticipated that, as more compounds are added to this library, predictions will become more accurate over a wider range of molecular attributes. Additionally, an expanded library may identify different/additional molecular descriptors that are correlated to dispersion potential. This may shed further light onto the specific structural properties responsible for the correlation to dispersion potential.

5. Conclusion

The ability to identify phase-separated co-solidified samples was afforded by implementing a combination of standard DSC and PDF transforms of PXRD patterns. Classification of co-solidified samples based on extent of miscibility enabled construction of a 12 compound library to model amorphous molecular solid dispersion potential. Logistic regression analysis of a molecular descriptor database identified a GETAWAY index highly correlated to solid dispersion potential. When the model was tested with external compounds possessing materials-properties spanning an appropriate variance space, successful predictions were made. The model developed herein is not universally applicable across all SMO compounds. The methodology presented outlines a novel approach to solving the complex issues surrounding API:polymer miscibility, where pharmaceutical sectors having large compound libraries at their disposal are poised to benefit from these materials-based models. Future work aims to increase interpretability of molecular indices to aid in understanding the complex phenomena associated with API:polymer miscibility requirements.

Acknowledgements

The authors would like to acknowledge a pre-doctoral fellowship from the American Foundation for Pharmaceutical Education. The authors would also like to thank Dr. David Engers for his continuous assistance and collaboration on this work.

References

Anon., 2002. Codessa Pro Software, University of Florida.

Anon., 2005. VCCLAB, Virtual Computational Chemistry Laboratory.

Allen, F.H., 2002. The Cambridge Structural Database: a quarter of a million crystal structures and rising. Acta Crystallogr. B 58, 380–388.

Chokshi, R., Zia, H., 2004. Hot-melt extrusion technique: a review. Iran. J. Pharm. Res. 3, 3–16.

Consonni, V., Todeschini, R., Pavan, M., 2002a. Structure/response correlations and similarity/diversity analysis by GETAWAY descriptors. 1. Theory of the novel 3D molecular descriptors. J. Chem. Inform. Comput. Sci. 42, 682–692.

Consonni, V., Todeschini, R., Pavan, M., Gramatica, P., 2002b. Structure/response correlations and similarity/diversity analysis by GETAWAY descriptors. 2. Application of the novel 3D molecular descriptors to QSAR/QSPR. J. Chem. Inform. Comput. Sci. 42, 693–705.

Couchman, P.R., Karasz, F.E., 1978. A classical thermodynamic discussion of the effect of composition on glass-transition temperatures. Macromolecules 11, 117–119.

Egami, T., Billinge, S.J.L., 2003. Underneath the Bragg Peaks, Structural analysis of Complex Materials. Elsevier, Oxford.

Estrada, E., 1996. Spectral moments of the edge adjacency matrix in molecular graphs. 1. Definition and applications to the prediction of physical properties of alkanes. J. Chem. Inform. Comput. Sci. 36, 844–849.

Friesen, D.T., Shanker, R., Crew, M., Smithey, D.T., Curatolo, W.J., Nightingale, J.A.S., 2008. Hydroxypropyl methylcellulose acetate succinate-based spray-dried dispersions: an overview. Mol. Pharm. 5, 1003–1019.

Gramatica, P., Corradi, M., Consonni, V., 2000. Modelling and prediction of soil sorption coefficients of non-ionic organic pesticides by molecular descriptors. Chemosphere 41, 763–777.

Hancock, B.C., Parks, M., 2000. What is the true solubility advantage for amorphous pharmaceuticals? Pharm. Res. 17, 397–404.

Huang, J., Wigent, R.J., Schwartz, J.B., 2008. Drug-polymer interaction and its significance on the physical stability of nifedipine amorphous dispersion in microparticles of an ammonio methacrylate copolymer and ethylcellulose binary blend. J. Pharm. Sci. 97, 251–262.

Ivanisevic, I., Bates, S., Chen, P., 2009. Novel methods for the assessment of miscibility of amorphous drug–polymer dispersions. J. Pharm. Sci. 98, 3373–3386.

Janssens, S., Roberts, C., Smith, E.F., Mooter, G.V.D., 2008. Physical stability of ternary solid dispersions of itraconazole in polyethyleneglycol 6000/hydroxypropylmethylcellulose 2910 E5 blends. Int. J. Pharm. 355, 100–107.

Janssens, S., Zeure, A.D., Paudel, A., Humbeeck, J.V., Rombaut, P., Mooter, G.V., online March, d., 2010. Influence of preparation methods on solid state supersaturation of amorphous solid dispersions: a case study with Itraconazole and Eudragit E100. Pharm. Res..

Kaushal, A.M., Gupta, P., Bansal, A.K., 2004. Amorphous drug delivery systems: molecular aspects, design, and performance. Crit. Rev. Ther. Drug Carrier Syst. 21, 133–193.

Kleinbaum, D.G., Klein, M., 2002. Logistic Regression, 2nd ed. Springer.

Kleinbaum, D.G., Kupper, L.L., Muller, K.E., Nizam, A., 1998. Applied Regression and other Multivariable Methods. Duxbury Press.

Marsac, P.J., Konno, H., Taylor, L.S., 2006a. A comparison of the physical stability of amorphous felodipine and nifedipine systems. Pharm. Res. 23, 2306–2316.

Marsac, P.J., Shamblin, S.L., Taylor, L.S., 2006b. Theoretical and practical approaches for prediction of drug-polymer miscibility and solubility. Pharm. Res. 23, 2417–2426.

Mihalic, Z., Trinajstic, N., 1992. A graph-theoretical approach to structure–property relationships. Symp. Graph Theory Chem. 69, 701–712.

Moore, M.D., Shi, Z., Wildfong, P.L.D., 2010. Structural interpretation in composite systems using powder X-ray diffraction: applications of error propagation to the pair distribution function. Pharm. Res..

Mooter, G.V.D., Wuyts, M., Blaton, N., Busson, R., Grobet, P., Augustijns, P., Kinget, R., 2001. Physical stabilisation of amorphous ketoconazole in solid dispersions with polyvinylpyrrolidone K25. Eur. J. Pharm. Sci. 12, 261–269.

Newman, A., Engers, D., Bates, S., Ivanisevic, I., Kelly, R.C., Zografi, G., 2008. Characterization of amorphous API:polymer mixtures using X-ray powder diffraction. J. Pharm. Sci. 97, 4840–4856.

Pampel, F.C., 2000. Logistic Regression: A Primer. Sage Publications.

Peterson, P.F., Bozin, E.S., Proffen, T., Billinge, S.J.L., 2003. Improved measures of quality for the atomic pair distribution function. J. Appl. Crystallogr. 36, 53–64.

Pregibon, D., 1981. Logistic regression diagnostics. Ann. Stat. 9, 705–724.

Prince, E., 2004. Mathematical Techniques in Crystallography and Materials Science, 3rd ed. Springer, New York.

Rumondor, A.C.F., Taylor, L.S., 2010. Effect of polymer hygroscopicity on the phase behavior of amorphous solid dispersions in the presence of moisture. Mol. Pharm. (available online January 2010).

Sekiguchi, K., Obi, N., 1961. Studies on absorption of eutectic mixtures. I. A comparison of the behavior of eutectic mixtures of sulphathiazole and that of ordinary sulphathiazole in man. Chem. Pharm. Bull. 9, 866–872.

Sethia, S., Squillante, E., 2004. Solid dispersion of carbamazepine in PVP K30 by conventional solvent evaporation and supercritical methods. Int. J. Pharm. 272, 1–10.

Six, K., Verreck, G., Peeters, J., Brewster, M., Mooter, G.V.D., 2004. Increased physical stability and improved dissolution properties of itraconazole, a class II drug, by solid dispersions that combine fast- and slow-dissolving polymers. J. Pharm. Sci. 93, 124–131.

Taylor, L.S., Zografi, G., 1997. Spectroscopic characterization of interactions between PVP and indomethacin in amorphous molecular dispersions. Pharm. Res. 14, 1691–1698.

Tetko, I.V., Gasteiger, J., Todeschini, R., Mauri, A., Livingstone, D., Ertl, P., Palyulin, V.A., Radchenko, E.V., Zefirov, N.S., Makarenko, A.S., Tanchuk, V.Y., Prokopenko, V.V., 2005. Virtual computational chemistry laboratory—design and description. J. Comput. Aided Mol. Des. 19, 453–463.

Thomas, I.R., Bruno, I.J., Cole, J.C., Macrae, C.F., Pidcock, E., Wood, P.A., 2010. WebCSD: the online portal to the Cambridge Structural Database. J. Appl. Crystallogr. 43, 362–366.

Todeschini, R., Consonni, V., 2002. Handbook of Molecular Descriptors. Wiley-VCH.

Waard, Hd., Hinrichs, W.L.J., Visser, M.R., Bologna, C., Frijlink, H.W., 2008. Unexpected differences in dissolution behavior of tablets prepared from solid dispersions with a surfactant physically mixed or incorporated. Int. J. Pharm. 349, 66–73.

Warren, B.E., 1990. X-ray Diffraction. Dover Publications, Inc., New York.

Waterbeemd, H.V.D., Gifford, E., 2003. ADMET in silico modelling: towards prediction paradise? Nat. Rev. Drug Discov. 2, 192–204.

Yoo, S.-U., Krill, S.L., Wang, Z., Telang, C., 2009. Miscibility/stability considerations in binary solid dispersion systems composed of functional excipients towards the design of multi-component amorphous systems. J. Pharm. Sci. 98, 4711–4723.